

# Chapter 4

## Degree of Freedom of a Mechanism

A mechanism consists of rigid bodies and of joints inter-connecting the bodies. A joint is a mechanical device which introduces kinematical constraints on the motion of the two bodies relative to each other. This implies that inter-connections by springs or dampers do not constitute joints since such elements do not create kinematical constraints. Two bodies cannot be connected by more than one joint. This means that the complete system of devices inter-connecting two bodies is counted as a single joint. A joint does not connect more than two bodies. If, for example,  $p > 2$  bodies are rotating about a single common shaft, this shaft represents  $p-1$  joints each of them connecting two bodies.

A single body moving in three-dimensional space without any kinematical constraint is said to have the degree of freedom  $F = 6$ . This is the minimal number of generalized coordinates required for specifying its position and angular orientation relative to some reference body. Let the moving body be connected to the reference body by a joint. Kinematical constraints introduced by this joint have the effect that the body has a degree of freedom  $1 \leq F \leq 5$ . This number  $F$  is also called *degree of freedom  $f$  of the joint*. The number of independent kinematical constraints in the joint is  $6 - f$ . Examples: Revolute, prismatic and helical joints have  $f = 1$ , cylindrical and universal joints have  $f = 2$ , and a spherical joint has  $f = 3$ . The degree of freedom is  $f = 4$  ( $f = 5$ ) if the spherical joint is free to move along a rigid line (in a rigid surface).

A mechanism is a joint-connected system of bodies. Let  $n$  be the number of bodies. One of the bodies is held fixed. In order to be connected the mechanism must have  $m \geq n - 1$  joints. Each joint  $i = 1, \dots, m$  has its individual degree of freedom  $1 \leq f_i \leq 5$ . The mechanism as a whole has a degree of freedom  $F$ . This is the minimal number of generalized coordinates required for specifying its position and angular orientation relative to the single body held fixed. The degree of freedom  $F$  depends not only on the numbers  $n$  and  $m$  and on the degrees of freedom  $1 \leq f_i \leq 5$  ( $i = 1, \dots, m$ ) of the

individual joints, but also on the structure of the system. This dependency is the subject of the present chapter.

## 4.1 Grübler's Formula

A mechanism with  $m = n - 1$  joints is said to have *tree structure* (Fig. 4.1a). Its characteristic feature is that any two bodies are connected by a uniquely determined chain of bodies and of joints. Examples are serial robot arms without kinematical constraint of the gripper to the surrounding environment and the human body when standing on one foot and with free hands. A mechanism with  $m = n$  joints contains a single closed chain or single loop. An example is shown in Fig. 4.1b. A single loop without side branches (the subsystem formed by the shaded bodies) is called *simple closed chain*. A mechanism with  $m > n$  joints is called *multiloop mechanism*. It is created by adding more joints in Fig. 4.1b. In both figures the schematically indicated joints are of arbitrary nature with individual degrees of freedom  $1 \leq f \leq 5$ .

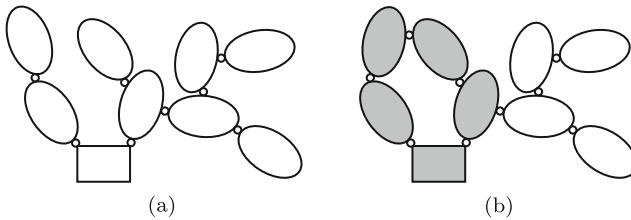


**Fig. 4.1** Mechanisms with tree structure ( $m = n - 1$ ) (a) and with a single closed chain ( $m = n$ ) (b). Simple closed chain formed by the shaded bodies

The degree of freedom  $F$  of a mechanism is determined as follows. As a preparatory step all joints of the mechanism are removed, so that all bodies except the single body held fixed are free of kinematical constraints. In this state these  $n - 1$  bodies have a total degree of freedom  $6(n - 1)$ , namely, six for each body. In joint  $i$  ( $i = 1, \dots, m$ ) with joint degree of freedom  $1 \leq f_i \leq 5$  there are  $6 - f_i$  kinematical constraints. The total number of constraints of all  $m$  joints equals the sum of all numbers  $(6 - f_i)$ . The total number of *independent* constraints may be smaller. It is smaller by  $d$  where  $d$  (defect) denotes the number of dependent constraints. After reconstituting the removed joints the degree of freedom of the mechanism is obtained:

$$F = 6(n - 1) - \left[ \sum_{i=1}^m (6 - f_i) - d \right] = 6(n - 1 - m) + d + \sum_{i=1}^m f_i \quad (1 \leq f_i \leq 5). \quad (4.1)$$

This formula is valid for all mechanisms. In theory as well as in engineering practice planar mechanisms and spherical mechanisms are important. In a planar mechanism each body is in plane motion, and the reference plane is the same for all bodies. In a spherical mechanism each body is rotating about a fixed point, and all bodies have the same fixed point. A simple example is the spherical four-bar with four bodies and four revolute joints intersecting at a single point. In planar motion as well as in spherical motion about a fixed point a single unconstrained body has the degree of freedom three. In planar as well as in spherical mechanisms an individual joint has the joint degree of freedom  $1 \leq f_i \leq 2$  and, consequently,  $3 - f_i$  constraints. In both types of mechanism the degree of freedom of the mechanism is

$$F = 3(n-1-m) + d + \sum_{i=1}^m f_i \quad (\text{planar and spherical mech's; } 1 \leq f_i \leq 2). \quad (4.2)$$

Planar mechanisms can be seen as special cases of spherical mechanisms. The fixed point common to all bodies is at infinity.

In the literature (4.1) and (4.2) are usually written without the defect  $d$ . These formulas are due to Grübler [3]. The formulas are accompanied by the warning that false results are obtained in the case of dependent constraints. A simple example shows that false results may be obtained even if the defect is taken into account. Imagine two systems 1 and 2 which are sharing a single body 0 which is held fixed. Suppose, (4.1) yields  $F_1 = -1$  for system 1 (indicating rigidity) and  $F_2 = 1$  for system 2. Clearly, the entire system composed of systems 1 and 2 together has the degree of freedom  $F = 1$ . However, (4.1) applied to the entire system yields the wrong result  $F = F_1 + F_2 = 0$  indicating rigidity. The formula  $F = F_1 + F_2$  is correct if and only if  $F_1, F_2 \geq 0$ . The general statement is: Equations (4.1) and (4.2) applied to an entire system yield correct results if and only if, by the same equations, every subsystem of the entire system has a degree of freedom  $\geq 0$ . Hence the conclusion: In order to get a correct result it is necessary, first, to determine the degree of freedom of subsystems. Every subsystem with a degree of freedom  $\leq 0$  must be counted as a single rigid body. Only then do (4.1) and (4.2) yield correct results for the entire system. Most engineering systems are so simple that the degree of freedom of subsystems is obvious without any analysis. In complex spatial multiloop systems, however, a separate analysis of subsystems may be necessary.

Equations (4.1) and (4.2) show that the degree of freedom  $F$  of a mechanism is independent of which body is chosen as fixed body.

Mechanisms with tree structure (Fig. 4.1a) are characterized by  $m = n - 1$  and  $d = 0$ . In this case, both formulas for the degree of freedom read

$$F = \sum_{i=1}^{n-1} f_i. \quad (4.3)$$

For mechanisms with a closed chain and, in particular, for the simple closed chain (Fig. 4.1b;  $m = n$ ) (4.1) and (4.2) have the forms

$$F = \begin{cases} -6 + d + \sum_{i=1}^n f_i & \text{(all mechanisms; } 1 \leq f_i \leq 5) \\ -3 + d + \sum_{i=1}^n f_i & \text{(planar and spherical mech's; } 1 \leq f_i \leq 2) . \end{cases} \quad (4.4)$$

A mechanism with degree of freedom  $F = 1$  is called 1-d.o.f. mechanism or mobility-one mechanism. From (4.4) follows

**Theorem 4.1.** *In a simple closed chain with mobility one and with independent constraints ( $F = 1$ ,  $d = 0$ ) the number of joint variables is*

$$\sum_{i=1}^n f_i = \begin{cases} 7 & \text{(nonspherical spatial simple closed chain)} \\ 4 & \text{(planar and spherical simple closed chains)} . \end{cases} \quad (4.5)$$

Applied to revolute joints ( $f_i \equiv 1$ ) this theorem states that a simple (nonspherical) spatial closed chain must have seven revolute joints and seven bodies in order to have mobility one if all constraints are independent. For planar and for spherical simple closed chains this number of revolute joints and of bodies is four. Engineering realizations are the planar four-bar and the spherical four-bar. For both of them the first Eq.(4.4) yields the correct result  $F = 1$  only if  $d = 3$ . Indeed, three constraints are dependent. In the planar four-bar, for example, one out of four parallel revolute joints establishes the constraint to the plane of motion. This constraint must not be counted as independent in the other three revolutes.

A mechanism is said to be *overconstrained* if it has a degree of freedom  $F \geq 1$  only because of the existence of dependent constraints ( $d > 0$ ). Overconstrained mechanisms must be manufactured with great precision because inaccuracies result in the loss of mobility. Inhomogeneous changes of temperature may have the same effect. For these reasons most engineering mechanisms are designed such that overconstraint does not occur. Example: The ideal planar four-bar is an overconstrained mechanism. This overconstraint is avoided by giving the bearing of one axis the freedom to adjust its direction as is required.

## 4.2 Illustrative Examples

The determination of the defect  $d$  in Grübler's Eq.(4.1) can be a difficult problem requiring a kinematics analysis in which all mechanism parameters – link lengths and parameters specifying directions of joint axes – are involved.

In the following sections this analysis is demonstrated for seven different mechanisms.

### 4.2.1 Five-Point-Contact Joint

Subject of investigation is a rigid body five points of which are constrained to move in prescribed surfaces. To be determined is the degree of freedom of the body. The five surfaces constitute a single body referred to as frame. The system is a mechanism with  $n = 2$  bodies and with  $m = 1$  joint. The constraint of a point  $P_i$  to a surface prevents the point from moving in the direction of the unit vector  $\mathbf{n}_i$  normal to the surface. There are five such constraints in the joint. If  $d$  is again the number of dependent constraints, the joint degree of freedom is  $f = 6 - (5 - d) = 1 + d$ . According to (4.1) this is also the degree of freedom of the mechanism and, thus, of the body.

The defect  $d$  is determined as follows. According to Chasles's Theorem 3.1 an infinitesimal displacement of a rigid body is a screw displacement with a certain screw axis and a certain pitch (this includes as special cases pure translation and pure rotation). The infinitesimal displacement of an arbitrary body-fixed point is directed along the helix through this point. Every line perpendicular to the helix is a complex line of the linear complex with this screw axis and with this pitch (see the comment on Fig. 2.5). From this it follows that the normals to the five surfaces at the points  $P_i$  ( $i = 1, \dots, 5$ ) are complex lines. Let  $\mathbf{r}_i$  ( $i = 1, \dots, 5$ ) be the position vectors of the points  $P_i$  in a reference basis fixed on the frame. In this basis the normals have Plücker vectors  $\mathbf{v}_i = \mathbf{n}_i$  and  $\mathbf{w}_i = \mathbf{r}_i \times \mathbf{n}_i$  ( $i = 1, \dots, 5$ ). From five *independent* complex lines the vectors  $\mathbf{a}$  and  $\mathbf{b}$  of a linear complex ( $\mathbf{a}; \mathbf{b}$ ) are determined by Eqs.(2.38):

$$\mathbf{w}_i \cdot \mathbf{a} + \mathbf{v}_i \cdot \mathbf{b} = 0 \quad (i = 1, \dots, 5). \quad (4.6)$$

The screw axis has the direction of  $\mathbf{a}$ . The location of the screw axis and the pitch are determined by (2.29):

$$\mathbf{u} = \frac{\mathbf{a} \times \mathbf{b}}{\mathbf{a}^2}, \quad p = \frac{\mathbf{a} \cdot \mathbf{b}}{\mathbf{a}^2}. \quad (4.7)$$

From these facts it follows that the defect  $d$  of the coefficient matrix in (4.6) is the quantity determining the degree of freedom  $f = 1 + d$  of the joint.

An engineering realization of the constraint of a body to five surfaces is shown in Fig. 4.2. The body, now called platform, is connected to a frame by five rods with spherical joints at both ends. Each surface is a sphere with the rod length as radius. The axes of the five rods are the complex lines. The platform on five rods finds an important engineering application in the five-point wheel suspension system for cars shown in Fig. 4.3. The platform is the

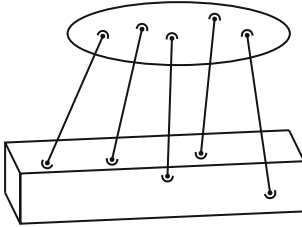


**Fig. 4.2** Platform mounted on five rods with spherical joints at both ends

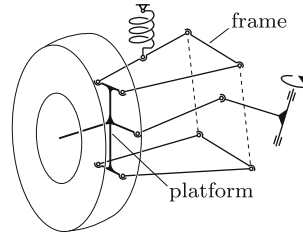


**Fig. 4.3** Five-point wheel suspension system

carrier of the wheel, and the frame is the car body. A single spherical joint on the car body is operated by the steering mechanism. When the steering is held fixed, the carrier has a single degree of freedom. Springs connecting the carrier with the car body allow small carrier displacements only. These displacements are screw displacements.

The screw displacement of a platform can be made visible by the following experiment. Instead of mounting the platform on rigid rods it is suspended by five mutually skew inextensible strings in such a way that an equilibrium position exists in which the weight of the platform keeps all strings tight. A small perturbation causes the platform to oscillate about the equilibrium position. This oscillation is a screw motion about the axis and with the pitch determined by (4.6) and (4.7).

If the rods in Fig. 4.2 are counted as bodies, the entire system is composed of  $n = 7$  bodies (fixed frame, platform and five rods) and of  $m = 10$  spherical joints each having the joint degree of freedom  $f = 3$ . With these numbers Grübler's formula (4.1) yields for the degree of freedom of the mechanism the result  $F' = 6(n - 1 - m) + d + mf = 6 + d$ . Since every rod has the degree of freedom of rotation about its own axis, the degree of freedom of the platform is  $F = F' - 5 = 1 + d$  as before.

To a platform mounted on five rods additional rods can be added in such a way that, in the assembly position, all rods are lines of a single linear complex. In this position then, the degree of freedom of the platform is  $F = 1$ . In general, it is not possible to move the platform into another position. The platform is said to be *shaky* in this position. In exceptional cases a platform is mounted on more than five rods in such a way that large motions are possible. This requires an arrangement where every position in the course of motion satisfies the condition that all rods are complex lines of a single linear complex. The platform-fixed endpoint of each rod is moving on the sphere having its center at the other endpoint of the rod. In Sect. 6.8 such systems are investigated.

### 4.2.2 Shaky Truss

In Fig. 4.4a a planar multiloop mechanism with  $n = 7$  bodies (fixed body 0 plus bodies 1, . . . , 6) and with  $m = 9$  revolute joints is shown (the connection of bodies 2, 4 and 5 represents two joints). To be determined is the degree of freedom  $F$ .

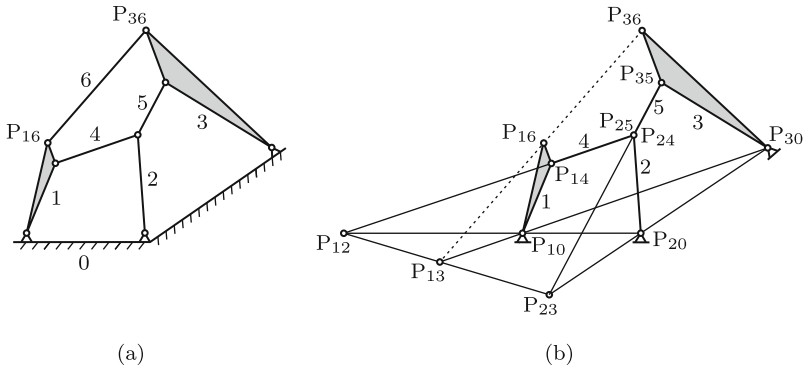


Fig. 4.4 Planar mechanism with 7 bodies and 9 revolute joints (a) before and (b) after eliminating rod 6

Solution: Equation (4.2) yields  $F = d$ . Hence the degree of freedom is  $F > 0$  only if at least one constraint is dependent. In order to find out whether this is the case, rod 6 is eliminated and, thereby, a single constraint forcing the endpoints  $P_{16}$  and  $P_{36}$  to have identical velocity components in the direction of rod 6. The mechanism without rod 6 is shown in Fig. 4.4b. If in this system with degree of freedom  $F = 1$   $P_{16}$  and  $P_{36}$  have identical velocity components in the direction of the eliminated rod 6, this rod 6 is unnecessary which means that  $d = 1$ . Velocities are determined with the help of Theorem 15.3 by Kennedy and Aronhold. The condition to be satisfied is that the pole  $P_{13}$  is located on the line  $\overline{P_{16}P_{36}}$ . This pole  $P_{13}$  is found as intersection of the lines  $\overline{P_{10}P_{30}}$  and  $\overline{P_{12}P_{23}}$ . The poles  $P_{12}$  and  $P_{23}$  are determined as intersections of the lines  $\overline{P_{10}P_{20}}$  and  $\overline{P_{14}P_{24}}$  and of the lines  $\overline{P_{20}P_{30}}$  and  $\overline{P_{25}P_{35}}$ , respectively. In the present case,  $P_{13}$  is, indeed, located on the line  $\overline{P_{16}P_{36}}$ . However, this is true only in the instantaneous position of the mechanism. Hence the conclusion: In the position shown the mechanism in Fig. 4.4a has the degree of freedom  $F = 1$ . Neighboring positions cannot be assumed. In statics the system is called an infinitesimally mobile or shaky truss. Grübler’s formula and the formula used for checking statical determinacy of trusses are directly related.

### 4.2.3 Closed Chain Formed by Four Planar Four-Bars

The planar system shown in Fig. 4.5 can be interpreted in different ways. For one thing, it is a multiloop system with  $m = 12$  bodies (the shaded bodies plus eight rods) and with  $n = 16$  revolute joints each joint having the individual degree of freedom  $f = 1$ . With these numbers Gr ubler's Eq.(4.2) yields the total degree of freedom  $F = d + 1$ . In a much simpler interpretation each pair of rods interconnecting two shaded bodies constitutes a joint with the individual degree of freedom  $f = 1$ . In this interpretation the system consists of bodies 1, 2, 3, 4 and of joints 1, 2, 3, 4. With these numbers Gr ubler's equation yields  $F = d + 1$  as before. In joint 1 the link lengths  $\ell_1, r_1, a_1, r_2$  represent a four-bar. Since the same is true for the other joints, the mechanism is formed by four coplanar four-bars. The link of length  $\ell_1$  in four-bar 1 is the fixed link. On this link the  $x, y$  reference system is fixed. The kinematics is analyzed as follows.

The links of lengths  $\ell_4$  and  $a_4$  are eliminated and thereby the constraints on the  $x, y$ -coordinates of the endpoints  $P_1, P_2, P_3, P_4$ :

$$(x_2 - x_1)^2 + (y_2 - y_1)^2 - \ell_4^2 = 0, \quad (x_4 - x_3)^2 + (y_4 - y_3)^2 - a_4^2 = 0. \quad (4.8)$$

The resulting system of four-bars 1, 2, 3 has the degree of freedom three. As independent variables the input angles  $\varphi_1, \varphi_2, \varphi_3$  of these four-bars are chosen. Figure 17.1 shows that a four-bar with input angle  $\varphi_i$  can assume two positions with output angles  $\psi_{i_1}$  and  $\psi_{i_2}$ . Their sines and cosines are determined by (17.12) and (17.11). For four-bar 1 the equations are

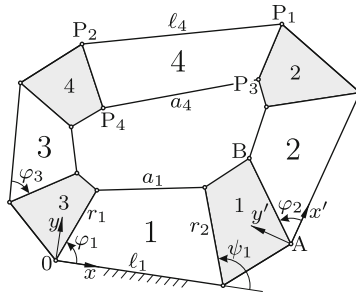


Fig. 4.5 Closed chain with planar four-bars 1, 2, 3, 4 connecting bodies 1, 2, 3, 4

$$\left. \begin{aligned} \cos \psi_{1_k} &= \frac{AC + (-1)^k B \sqrt{A^2 + B^2 - C^2}}{A^2 + B^2}, \\ \sin \psi_{1_k} &= \frac{BC - (-1)^k A \sqrt{A^2 + B^2 - C^2}}{A^2 + B^2} \end{aligned} \right\} (k = 1, 2), \quad (4.9)$$



$$\left. \begin{aligned} A &= 2r_2(\ell_1 - r_1 \cos \varphi_1), & B &= -2r_1r_2 \sin \varphi_1, \\ C &= 2r_1\ell_1 \cos \varphi_1 - (r_1^2 + \ell_1^2 + r_2^2 - a_1^2). \end{aligned} \right\} \quad (4.10)$$

The  $x, y$ -coordinates of the points A and B in these two positions are expressed in terms of  $\ell_1, r_2, \cos \psi_{1_k}, \sin \psi_{1_k}$  and of parameters specifying body 1.

The same equations, but with  $\varphi_2$  as independent variable and with other parameters, determine the coordinates of P<sub>1</sub> and P<sub>3</sub> in the  $x', y'$ -system shown in the figure. As before, two different solutions exist for every angle  $\varphi_2$ . Transformation from the  $x', y'$ -system into the  $x, y$ -system results in expressions for the  $x, y$ -coordinates of P<sub>1</sub> and P<sub>3</sub> as functions of  $\varphi_1$  and  $\varphi_2$ . Next, the  $x, y$ -coordinates of P<sub>2</sub> and P<sub>4</sub> are expressed as functions of  $\varphi_1$  and  $\varphi_3$ . With minor modifications the equations are the same as for the coordinates of P<sub>1</sub> and P<sub>3</sub>.

The results obtained so far are summarized as follows. Four different sets of  $x, y$ -coordinates of P<sub>2</sub> and P<sub>4</sub> are known as functions of  $\varphi_1$  and  $\varphi_3$ , and four different sets of  $x, y$ -coordinates of P<sub>1</sub> and P<sub>3</sub> are known as functions of  $\varphi_1$  and  $\varphi_2$ . Each of the former four sets has to be combined with each of the latter four sets. Thus, altogether sixteen combinations have to be investigated. For each combination Eqs. (4.8) are formulated. For at least one combination the degree of freedom is either  $F = 1$  or  $F = 2$ . It is  $F = 1$  if for every  $\varphi_1$  (in a certain interval) unique real solutions  $\varphi_2, \varphi_3$  exist. It is  $F = 2$  if both constraint equations are identical. A combination has the degree of freedom  $F = 0$  if real solutions  $\varphi_2, \varphi_3$  do not exist for any angle  $\varphi_1$ .

#### 4.2.4 Trihedral Plane-Symmetric Bricard Mechanism

The mechanism shown in Fig. 4.6 is a spatial closed chain with six bodies (fixed body 0 and bodies 1, ..., 5) and with six revolute joints 1, ..., 6. The two joint axes of each body are mutually orthogonal and nonintersecting. Bodies 0, 2 and 4 are identical and bodies 1, 3 and 5 are identical. Furthermore, body 1 is a mirror image of body 0. In the position shown the bodies are inscribed in a cube with all joint axes and all common perpendiculars of adjacent joint axes aligned along edges of the cube. In this cube configuration the joint axes 1, 3, 5 form a trihedral intersecting at a single point, and the axes 2, 4, 6 form another trihedral. Furthermore, the six axes display a triple plane-symmetry. They are symmetric with respect to the plane spanned by the axes 1 and 4, to the plane spanned by the axes 2 and 5 and to the plane spanned by the axes 3 and 6.

The kinematics of the mechanism is best understood if a model is available. It can be produced from cardboard by folding bodies. The angle  $\gamma$  should be 30°. From such a model it is learned that the mechanism has the

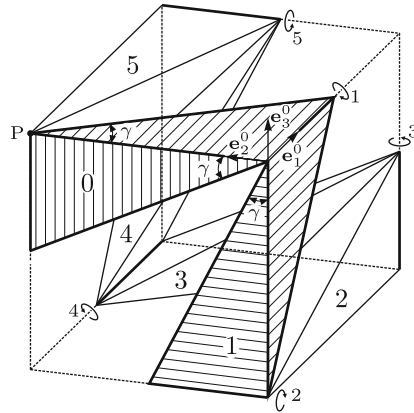


Fig. 4.6 Spatial closed chain with six bodies and six revolute joints

degree of freedom  $F = 1$ . Moreover, the axes  $1, 3, 5$  and  $2, 4, 6$  are permanently forming two trihedrals and also the triple plane-symmetry is preserved. These experimental results are confirmed by the following kinematics analysis (Wittenburg [7, 8]).

Equation (4.1) yields  $F = d$ . Hence a degree of freedom  $F > 0$  exists only if at least one constraint is dependent. According to Grübler’s formula there are altogether 30 constraints in the altogether six joints. It is not necessary to analyze this system of constraints. The kinematics analysis is much simpler if the joint between bodies 0 and 5 is cut. This results in a serial open chain with five joints. For this chain Grübler’s formula (4.3) yields the degree of freedom  $F = 5$ . Reconstitution of the cut joint introduces five constraints. These are the constraints which have to be analyzed. This is done as follows. On each body  $i$  ( $i = 0, \dots, 5$ ) a body-fixed basis  $\underline{e}^i$  is defined. In Fig. 4.6 only basis  $\underline{e}^0$  is shown. In the cube configuration of this figure all body-fixed bases are aligned parallel. The locations of the origins are without interest. Three of the five constraint equations express the fact that, independent of rotation angles in the joints, the chain of vectors leading from the point P on body 0 along body edges to the coincident point P on body 5 is closed. This is the vector equation

$$-\underline{e}_2^0 - \underline{e}_3^1 + \underline{e}_1^2 + \underline{e}_2^3 + \underline{e}_3^4 - \underline{e}_1^5 = \mathbf{0}. \tag{4.11}$$

Two more constraint equations express the fact that the vectors  $\underline{e}_1^5$  and  $\underline{e}_2^5$  are both orthogonal to  $\underline{e}_3^0$ :

$$\underline{e}_1^5 \cdot \underline{e}_3^0 = 0, \quad \underline{e}_2^5 \cdot \underline{e}_3^0 = 0. \tag{4.12}$$

In order to obtain five scalar constraint equations the vectors must be decomposed in a common basis. For this purpose joint variables are defined as

follows. In joint  $i$  ( $i = 1, \dots, 5$ )  $\varphi_i$  is the rotation angle of body  $i$  relative to body  $i - 1$ . Sign convention:  $\varphi_1, \varphi_2, \varphi_3$  are positive and  $\varphi_4, \varphi_5$  are negative in the case of a right-handed rotation about the basis vector in the respective joint axis. In the cube configuration all angles are zero. Let  $\underline{A}_i$  be the transformation matrix for joint  $i$  defined by the equation  $\underline{\mathbf{e}}^i = \underline{A}_i \underline{\mathbf{e}}^{i-1}$ . With the abbreviations  $c_i = \cos \varphi_i, s_i = \sin \varphi_i$  these matrices are

$$\begin{aligned} \underline{A}_1 = & & \underline{A}_2 = & & \underline{A}_3 = & & \underline{A}_4 = & & \underline{A}_5 = \\ \begin{bmatrix} 1 & 0 & 0 \\ 0 & c_1 & s_1 \\ 0 & -s_1 & c_1 \end{bmatrix}, & \begin{bmatrix} c_2 & 0 & -s_2 \\ 0 & 1 & 0 \\ s_2 & 0 & c_2 \end{bmatrix}, & \begin{bmatrix} c_3 & s_3 & 0 \\ -s_3 & c_3 & 0 \\ 0 & 0 & 1 \end{bmatrix}, & \begin{bmatrix} 1 & 0 & 0 \\ 0 & c_4 & -s_4 \\ 0 & s_4 & c_4 \end{bmatrix}, & \begin{bmatrix} c_5 & 0 & s_5 \\ 0 & 1 & 0 \\ -s_5 & 0 & c_5 \end{bmatrix}. \end{aligned} \quad (4.13)$$

The coordinate transformations for (4.11) and (4.12) are simplest if all vectors are decomposed either in basis  $\underline{\mathbf{e}}^2$  or in  $\underline{\mathbf{e}}^3$ . With  $\underline{\mathbf{e}}^3$  (4.11) takes the form

$$\underline{A}_3 \underline{A}_2 \underline{A}_1 \begin{bmatrix} 0 \\ -1 \\ 0 \end{bmatrix} + \underline{A}_3 \underline{A}_2 \begin{bmatrix} 0 \\ 0 \\ -1 \end{bmatrix} + \underline{A}_3 \begin{bmatrix} 1 \\ 0 \\ 0 \end{bmatrix} + \begin{bmatrix} 0 \\ 1 \\ 0 \end{bmatrix} + \underline{A}_4^T \begin{bmatrix} 0 \\ 0 \\ 1 \end{bmatrix} + \underline{A}_4^T \underline{A}_5^T \begin{bmatrix} -1 \\ 0 \\ 0 \end{bmatrix} = \begin{bmatrix} 0 \\ 0 \\ 0 \end{bmatrix}. \quad (4.14)$$

These equations are

$$c_3[1 + s_2(1 - s_1)] - s_3 c_1 - c_5 = 0, \quad (4.15)$$

$$s_3[1 + s_2(1 - s_1)] + c_3 c_1 - s_4(1 - s_5) - 1 = 0, \quad (4.16)$$

$$c_2(1 - s_1) - c_4(1 - s_5) = 0. \quad (4.17)$$

Also the scalar products in (4.12) are expressed in terms of vector coordinates in  $\underline{\mathbf{e}}^3$ . This yields the equations

$$c_5(-c_3 s_2 c_1 + s_3 s_1) + s_5[s_4(s_3 s_2 c_1 + c_3 s_1) + c_4 c_2 c_1] = 0, \quad (4.18)$$

$$c_4(s_3 s_2 c_1 + c_3 s_1) - s_4 c_2 c_1 = 0. \quad (4.19)$$

From experimenting with the cardboard model it is learned that in every position of the mechanism the constraint equations are satisfied:

$$\varphi_3 = \varphi_1, \quad \varphi_5 = \varphi_1, \quad \varphi_4 = \varphi_2. \quad (4.20)$$

When this is substituted, (4.15) – (4.19) become

$$\left. \begin{aligned} c_1(s_1 + s_1 s_2 - s_2) &= 0, \\ (s_1 - 1)(s_1 + s_1 s_2 - s_2) &= 0, \\ 0 &= 0, \\ c_1(1 + s_1 + s_1 s_2)(s_1 + s_1 s_2 - s_2) &= 0, \\ c_1 c_2(s_1 + s_1 s_2 - s_2) &= 0. \end{aligned} \right\} \quad (4.21)$$

These equations are satisfied if  $s_1 + s_1 s_2 - s_2 = 0$ . This is the equation

$$\sin \varphi_2 = \frac{\sin \varphi_1}{1 - \sin \varphi_1}. \quad (4.22)$$

In addition to (4.20) this constitutes a fourth independent constraint equation. There are no other independent constraint equations. Hence the mechanism is overconstrained with the degree of freedom  $F = 1$ . As independent variable the angle  $\varphi_1$  is chosen.

Remark: The constraint Eqs.(4.20) can be found without making experiments as follows. Multiply (4.16) by  $c_1c_4$ , (4.17) by  $-c_1s_4$ , (4.19) by  $-(1 - s_1)$  and add. Simple reformulation followed by division through  $c_4$  results in an equation relating  $\varphi_3$  to  $\varphi_1$ :

$$(1 - s_1)c_3 = (1 - s_3)c_1 . \tag{4.23}$$

The equation has the solutions  $\varphi_3 = \varphi_1$  and  $\varphi_3 = \pi/2$ . Only the first solution is useful. This is the first Eq.(4.20). Because of the equal character of all bodies and of all joints and because of the definitions of joint angles this equation holds true if the indices are increased by 1 and by 2. This yields the other two constraint equations  $\varphi_4 = \varphi_2$  and  $\varphi_5 = \varphi_3$ . End of remark.

The relationship (4.22) is illustrated in the diagram of Fig. 4.7. Because of the conditions  $|\sin \varphi_{1,2}| \leq 1$  the angles are restricted to the intervals  $-210^\circ \leq \varphi_1 \leq +30^\circ$  and  $-30^\circ \leq \varphi_2 \leq +210^\circ$ . Motion in these intervals is possible without collision of neighboring bodies if the angle  $\gamma$  shown in Fig. 4.6 is  $\gamma \leq 30^\circ$ . The mechanism can undergo a continuous twisting motion similar to an elastic ribbon.

Differentiation of (4.22) with respect to time yields the relationship between angular velocities:

$$\dot{\varphi}_2 = \dot{\varphi}_1 \frac{\cos \varphi_1}{(1 - \sin \varphi_1)^2 \cos \varphi_2} = \dot{\varphi}_1 \frac{\cos \varphi_1}{(1 - \sin \varphi_1)\sqrt{1 - 2 \sin \varphi_1}} . \tag{4.24}$$

Differentiating one more time produces for the angular acceleration the expression

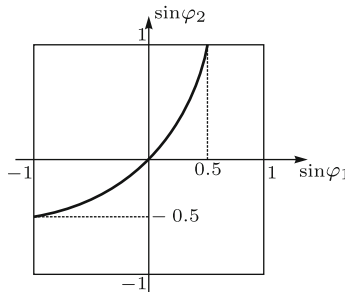


Fig. 4.7 Relationship between  $\varphi_1$  and  $\varphi_2$  in Fig. 4.6

$$\ddot{\varphi}_2 = \ddot{\varphi}_1 \frac{\cos \varphi_1}{(1 - \sin \varphi_1)\sqrt{1 - 2 \sin \varphi_1}} + \dot{\varphi}_1^2 \frac{2 - 2 \sin \varphi_1 - \sin^2 \varphi_1}{(1 - \sin \varphi_1)(1 - 2 \sin \varphi_1)^{3/2}}. \quad (4.25)$$

The mechanism is highly special. A mechanism having two trihedrals of permanently intersecting axes need not be plane-symmetric, and a plane-symmetric mechanism need not be trihedral. Bricard [1] discovered a five-parametric family of trihedral mechanisms and an eight-parametric family of plane-symmetric mechanisms. These mechanisms are analyzed in Sects. 6.4.2 and 6.4.3.

### 4.2.5 Line-Symmetric Bricard Mechanism

The mechanism shown in Fig. 4.8 is another spatial closed chain with six bodies (fixed body 0 and bodies 1, . . . , 5) and with six revolute joints 1, . . . , 6 (thick lines). The two joint axes of each body are mutually orthogonal and intersecting. In the position shown the axes are edges of a cube (dashed lines). The name of the mechanism points to the fact that the six joint axes are pairwise symmetric with respect to a line (pairs 1 and 4, 2 and 5, 3 and 6). In the cube configuration the line of symmetry is identified as follows. Draw in the square at the bottom of the cube the diagonal through P and give this diagonal a vertical translation by half the side length of the cube. It is obvious that a 180°-rotation about the line thus defined carries joint axis  $i$  ( $i = 1, 2, 3$ ) into the position originally held by joint axis  $i + 3$ .

A kinematics analysis is found in Pandrea [5]<sup>1</sup>. For checking results it is helpful to have a model made of six identical pieces of cardboard.

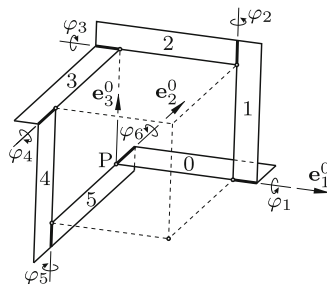


Fig. 4.8 Spatial closed chain with six bodies and six revolute joints

<sup>1</sup> Pandrea attributes the mechanism to Franke. In a private communication P. Dietmaier pointed out that *R. Franke: Vom Aufbau der Getriebe, v.2 (1951) Deutscher-Ingenieur-Verlag Düsseldorf* shows, without kinematics analysis, a line-symmetric mechanism in which the joint axes on the bodies are skew.

Equation (4.1) yields  $F = d$ . Hence a degree of freedom  $F > 0$  exists only if at least one constraint is dependent. Constraint equations are formulated by a method similar to the one used in the previous section. On each body  $i$  ( $i = 0, \dots, 5$ ) a body-fixed basis  $\underline{e}^i$  is defined. In Fig. 4.8 only basis  $\underline{e}^0$  is shown. In the position shown in this figure all body-fixed bases are aligned parallel. Three of the five constraint equations express the fact that, independent of rotation angles in the joints, the chain of vectors leading from the point P on body 0 along body edges to the coincident point P on body 5 is closed. This is the constraint equation

$$\underline{e}_1^0 + \underline{e}_3^1 - \underline{e}_1^2 - \underline{e}_2^3 - \underline{e}_3^4 + \underline{e}_2^5 = \mathbf{0}. \quad (4.26)$$

Let  $\underline{A}_i$  be the transformation matrix in the relationship  $\underline{e}^i = \underline{A}_i \underline{e}^{i-1}$  ( $i = 0, \dots, 5$  cyclic). The matrices satisfy the constraint equation  $\underline{A}_6 \underline{A}_5 \underline{A}_4 \underline{A}_3 \underline{A}_2 \underline{A}_1 = \underline{I}$  or

$$\underline{A}_3 \underline{A}_2 \underline{A}_1 = (\underline{A}_6 \underline{A}_5 \underline{A}_4)^T. \quad (4.27)$$

Every matrix  $\underline{A}_i$  is a function of the rotation angle  $\varphi_i$  of the respective joint  $i$ . Definition:  $\varphi_i$  is the rotation angle of body  $i$  relative to body  $i-1$  ( $i = 1, \dots, 5$ ) and of body 0 relative to body 5 in the case  $i = 6$ . Sign convention:  $\varphi_1, \varphi_2, \varphi_4$  are positive and  $\varphi_3, \varphi_5, \varphi_6$  are negative in the case of a right-handed rotation about the basis vector in the respective joint axis. In the configuration shown in the figure all angles are zero. With the abbreviations  $c_i = \cos \varphi_i$ ,  $s_i = \sin \varphi_i$  the matrices are

$$\left. \begin{aligned} \underline{A}_3 &= \begin{bmatrix} 1 & 0 & 0 \\ 0 & c_3 & -s_3 \\ 0 & s_3 & c_3 \end{bmatrix}, & \underline{A}_2 &= \begin{bmatrix} c_2 & s_2 & 0 \\ -s_2 & c_2 & 0 \\ 0 & 0 & 1 \end{bmatrix}, & \underline{A}_1 &= \begin{bmatrix} 1 & 0 & 0 \\ 0 & c_1 & s_1 \\ 0 & -s_1 & c_1 \end{bmatrix}, \\ \underline{A}_6 &= \begin{bmatrix} c_6 & 0 & s_6 \\ 0 & 1 & 0 \\ -s_6 & 0 & c_6 \end{bmatrix}, & \underline{A}_5 &= \begin{bmatrix} c_5 & -s_5 & 0 \\ s_5 & c_5 & 0 \\ 0 & 0 & 1 \end{bmatrix}, & \underline{A}_4 &= \begin{bmatrix} c_4 & 0 & -s_4 \\ 0 & 1 & 0 \\ s_4 & 0 & c_4 \end{bmatrix}. \end{aligned} \right\} \quad (4.28)$$

With these expressions (4.27) becomes

$$\begin{aligned} & \begin{bmatrix} c_2 & c_1 s_2 & s_1 s_2 \\ -s_2 c_3 & c_1 c_2 c_3 + s_1 s_3 & s_1 c_2 c_3 - c_1 s_3 \\ -s_2 s_3 & c_1 c_2 s_3 - s_1 c_3 & s_1 c_2 s_3 + c_1 c_3 \end{bmatrix} \\ &= \begin{bmatrix} c_4 c_5 c_6 + s_4 s_6 & c_4 s_5 & -c_4 c_5 s_6 + s_4 c_6 \\ -s_5 c_6 & c_5 & s_5 s_6 \\ -s_4 c_5 c_6 + c_4 s_6 & -s_4 s_5 & s_4 c_5 s_6 + c_4 c_6 \end{bmatrix}. \end{aligned} \quad (4.29)$$

Following Pandrea the identity of matrix elements is formulated. The elements (1,2) and (2,1) yield the equations  $c_1 s_2 = c_4 s_5$  and  $c_3 s_2 = c_6 s_5$ . They are satisfied with

$$c_4 = c_1, \quad s_5 = s_2, \quad c_6 = c_3, \quad (4.30)$$

but also with  $c_4 = -c_1$ ,  $s_5 = -s_2$ ,  $c_6 = -c_3$ . In either case the signs of  $s_4$ ,  $c_5$  and  $s_6$  are still unknown. The calculations to come reveal that the pairwise identity of all matrix elements is possible only if Eqs.(4.30) are valid in combination with

$$s_4 = -s_1, \quad c_5 = c_2, \quad s_6 = -s_3. \quad (4.31)$$

Hence

$$\varphi_4 = -\varphi_1, \quad \varphi_5 = \varphi_2, \quad \varphi_6 = -\varphi_3. \quad (4.32)$$

After substituting (4.30) and (4.31) into (4.29) the pairwise identity of the matrix elements (1,1) and (3,1) is formulated. This produces the equations

$$\left. \begin{aligned} c_1 c_2 c_3 + s_1 s_3 &= c_2, \\ s_1 c_2 c_3 + (s_2 - c_1) s_3 &= 0. \end{aligned} \right\} \quad (4.33)$$

Resolving for  $c_3$  and  $s_3$  results in

$$c_3 = \frac{c_1 - s_2}{1 - c_1 s_2}, \quad s_3 = \frac{s_1 c_2}{1 - c_1 s_2}. \quad (4.34)$$

By substituting these expressions the pairwise identity of all matrix elements in (4.29) is verified.

Next, (4.26) is decomposed in basis  $\underline{e}^3$ . Using, for the moment, in (4.28) only (4.30) and (4.31) this decomposition produces the equations

$$c_2 + c_1 s_2 = 1 - s_1, \quad (4.35)$$

$$c_2 - c_3 s_2 = 1 + s_3, \quad c_3 - s_2 s_3 = c_1 - s_1 s_2. \quad (4.36)$$

When in (4.36)  $c_3$  and  $s_3$  are replaced by the expressions (4.34), these two equations are satisfied if (4.35) is satisfied. This proves the existence of a single dependent constraint. Thus, the mechanism is an overconstrained mechanism with the degree of freedom  $F = 1$ . Equation (4.35) has two solutions

$$\left. \begin{aligned} c_{2_k} &= \frac{1 - s_1 + (-1)^k c_1 \sqrt{1 + 2s_1(1 - s_1)}}{1 + c_1^2}, \\ s_{2_k} &= \frac{c_1(1 - s_1) - (-1)^k \sqrt{1 + 2s_1(1 - s_1)}}{1 + c_1^2} \end{aligned} \right\} (k = 1, 2). \quad (4.37)$$

With each solution Eqs.(4.34) yield the corresponding solution  $\varphi_{3_k}$ . Equations (4.32) yield the remaining angles. The two pairs of solutions  $\varphi_3$ ,  $\varphi_2$  are related through the equations

$$\varphi_{3_k} = \varphi_{2_j} - \frac{\pi}{2} \quad (k, j = 1, 2; k \neq j). \quad (4.38)$$

This is proved by substituting (4.37) into (4.34) and by verifying that  $c_{3k} = s_{2j}$  and  $s_{3k} = -c_{2j}$ .

The square root in (4.37) is zero for  $s_1 = (1 - \sqrt{3})/2$ , i.e. for  $\varphi_{\min} \approx -21,5^\circ$  and for  $\varphi_{\max} \approx \pi + 21,5^\circ$ . Only if  $\varphi_1$  is in the interval between these bounds, the angle  $\varphi_2$  is real. At the bounds the solution is  $c_2 = \sqrt{3}-1$ . This determines the angles  $\varphi_2 \approx \pm 42,9^\circ$ . In the diagram in Fig. 4.9  $\varphi_{2k}$  and  $\varphi_{3k}$  ( $k = 1, 2$ ) are shown as functions of  $\varphi_1$ . The mechanism can be assembled in two configurations. The change from one configuration to the other is achieved by opening and re-closing a single joint in such a way that body-fixed vectors along the opened joint axis have equal directions after if they have equal directions before. In Fig. 4.8 the first configuration is shown for the variable  $\varphi_1 = 0$  with  $\varphi_2 = \dots = \varphi_5 = 0$ . In the second configuration  $\varphi_1 = 0$  is associated with  $\varphi_3 = -\pi/2$ ,  $\varphi_4 = 0$ ,  $\varphi_2 = \varphi_5 = \varphi_6 = \pi/2$ . This configuration is shown in Fig. 4.10a. It is possible to open and to re-close a single joint in such a way that the said body-fixed vectors along the joint axis reverse their relative orientation. However, this re-closing is possible in a single position only in which the system is then rigid. This position is shown in Fig. 4.10b.

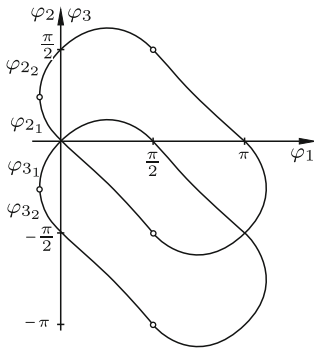


**Fig. 4.9** Angles  $\varphi_{2k}$  and  $\varphi_{3k}$  ( $k = 1, 2$ ) as functions of  $\varphi_1$

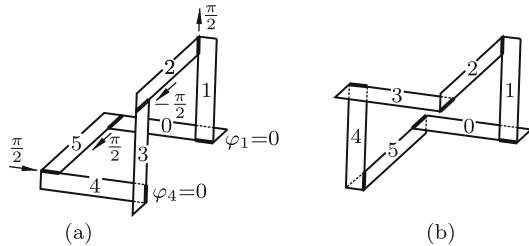


**Fig. 4.10** Second mobile configuration (a) and rigid configuration (b)

Angular velocities: From (4.32) and (4.38) it follows that  $\dot{\varphi}_4 = -\dot{\varphi}_1$ ,  $\dot{\varphi}_5 = \dot{\varphi}_2$ ,  $\dot{\varphi}_6 = -\dot{\varphi}_3$  and  $\dot{\varphi}_{3k} = \dot{\varphi}_{2j}$  ( $k, j = 1, 2; k \neq j$ ). Therefore, it suffices to express  $\dot{\varphi}_2$  in terms of  $\dot{\varphi}_1$  and  $\varphi_1$ . Implicit differentiation of (4.35) in combination with (4.37) yields

$$\begin{aligned} \dot{\varphi}_{2k} &= \dot{\varphi}_1 \frac{s_1 s_{2k} - c_1}{c_1 c_{2k} - s_{2k}} \\ &= -\dot{\varphi}_1 \frac{(-1)^k c_1 (2 - s_1) + s_1 \sqrt{1 + 2s_1(1 - s_1)}}{(1 + c_1^2) \sqrt{1 + 2s_1(1 - s_1)}} \quad (k = 1, 2). \end{aligned} \quad (4.39)$$



The mechanism is a very special case of a nine-parametric family of line-symmetric Bricard mechanisms. These mechanisms are analyzed in Sect. 6.4.1.

### 4.2.6 Homokinetic Shaft Coupling

The mechanism shown in Fig. 4.11 is a spatial simple closed chain  $S_1R_1S_2R_2$  with an additional revolute joint  $R_3$ . The parameters are such that, in the position shown, the closed chain is symmetric with respect to the plane  $\Sigma$  which is bisecting the angle between links 1 and 2 (referred to as shafts 1 and 2) and containing  $S_1, S_2$  and the point of intersection A of the revolutes  $R_1$  and  $R_2$  (in the figure  $\Sigma$  is normal to the plane of the drawing). For the entire mechanism with five bodies  $0, \dots, 4$  and with five joints Gr ubler's Eq.(4.4) yields the degree of freedom  $F = 3$ . Shaft 2 is free to change its direction in space as is indicated by arrows. In addition, shaft 1 is free to rotate about its longitudinal axis (angle of rotation  $\varphi_1$ ). In every position of the mechanism the closed chain is symmetric with respect to the plane  $\Sigma$  bisecting the angle between shafts 1 and 2 and containing  $S_1, S_2$  and A. When the direction of shaft 2 is fixed,  $\Sigma$  is fixed independent of  $\varphi_1$ . Permanent symmetry with respect to a fixed plane  $\Sigma$  has the consequence that both shafts have identical angular velocities:  $\dot{\varphi}_2 \equiv \dot{\varphi}_1$ . The results are summarized as follows. The plane-symmetric closed chain is a shaft coupling characterized by the properties

(A) the axis of shaft 2 is free to change its direction during operation

(B)  $\dot{\varphi}_2/\dot{\varphi}_1 \equiv 1$  independent of  $\varphi_1$  in every position of shaft 2 held fixed.

Shaft couplings having these two properties are called homokinetic. The combination of these properties is essential in many engineering systems. A typ-

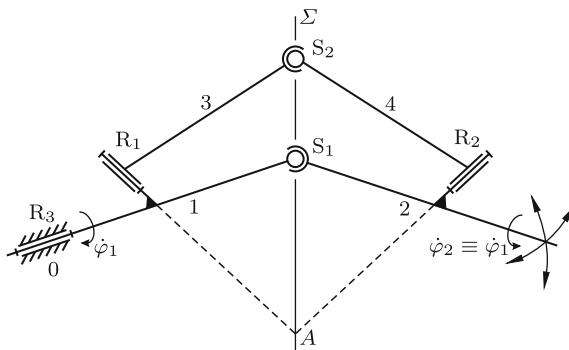


Fig. 4.11 Homokinetic shaft coupling with a plane-symmetric closed chain  $S_1R_1S_2R_2$

ical example is the coupling between front wheel and drive shaft in a front-wheel driven automobile. The coupling must have property (A) since the direction of the wheel axis is changing due to steering maneuvers and to dynamic processes in the suspension system. Property (B) is necessary in order to prevent resonance vibrations in the car. The well-known Hooke's joint is a shaft coupling having property (A), but not property (B). Its ratio  $\dot{\varphi}_2/\dot{\varphi}_1$  is a  $\pi$ -periodic function of  $\varphi_1$ . Only its mean value is 1. This is shown in Sect. 13.1. In the power train of a car such a source of vibrations with a frequency proportional to the speed of the car is unacceptable. It was the need for cars with front-wheel drive which triggered the development of compact and reliable homokinetic shaft couplings. See Sect. 13.4 for a more general theory.

### 4.2.7 Mobile Tilings

In Fig. 4.12a  $Q$  is a convex quadrilateral of arbitrary nonparallelogram-shape. By  $180^\circ$ -rotations about the midpoints of its sides four congruent quadrilaterals are produced. Let  $Q'$  be one of them, and let  $\mathbf{t}_1$  and  $\mathbf{t}_2$  be the two diagonals as shown. By repeated translations  $\mathbf{t}_1$  and  $\mathbf{t}_2$  of the hexagon composed of  $Q$  and  $Q'$  the infinite plane is filled with congruent quadrilaterals without gaps and overlaps. The individual quadrilateral is referred to as tile, and the plane-filling pattern is called tiling. The tiling is invariant with respect to periodical translations with  $\mathbf{t}_1$ ,  $\mathbf{t}_2$ ,  $\mathbf{t}_1 + \mathbf{t}_2$  and  $\mathbf{t}_1 - \mathbf{t}_2$ . It is also invariant with respect to  $180^\circ$ -rotations about the midpoints of sides of quadrilaterals.

Remark: All statements made up to this point are valid also for parallelograms and for nonconvex quadrilaterals. They are also valid in the much more general case when each side of  $Q$  is replaced by an arbitrary centrally symmetric curve. More about tilings is found in Sect. 14.6.

Kokotsakis [4] recognized that a tiling made of convex quadrilaterals of arbitrary nonparallelogram-shape is a 1-d.o.f. mechanism if all quadrilaterals are rigid bodies and all sides revolute joints.

Proof (Stachel [6]): The shaded area in Fig. 4.12b is a cluster of four congruent quadrilaterals  $Q_1$ ,  $Q_2$ ,  $Q_3$ ,  $Q_4$  grouped around center  $O_1$ . In what follows, it is referred to as cluster 1. When it is isolated from the surrounding quadrilaterals, it represents a spherical four-bar with constant angles  $\alpha_1$ ,  $\alpha_2$ ,  $\alpha_3$ ,  $\alpha_4$  and with axes along unit vectors  $\mathbf{n}_1$ ,  $\mathbf{n}_2$ ,  $\mathbf{n}_3$ ,  $\mathbf{n}_4$  pointing away from  $O_1$ . Notation:  $\alpha_i$  ( $i = 1, 2, 3, 4$ ) is the internal angle of  $Q_i$  at  $O_1$ . The variable angle of rotation of  $Q_i$  relative to  $Q_{i-1}$  about  $\mathbf{n}_i$  is called  $\varphi_i$  ( $i = 1, 2, 3, 4$  cyclic;  $\varphi_i = 0$  in the planar position). This is the notation used in Fig. 18.1a. For a given angle  $\varphi_1$  the spherical four-bar can assume two positions. Two solutions  $\varphi_4$  as functions of  $\varphi_1$  are determined by Eqs.(18.2),

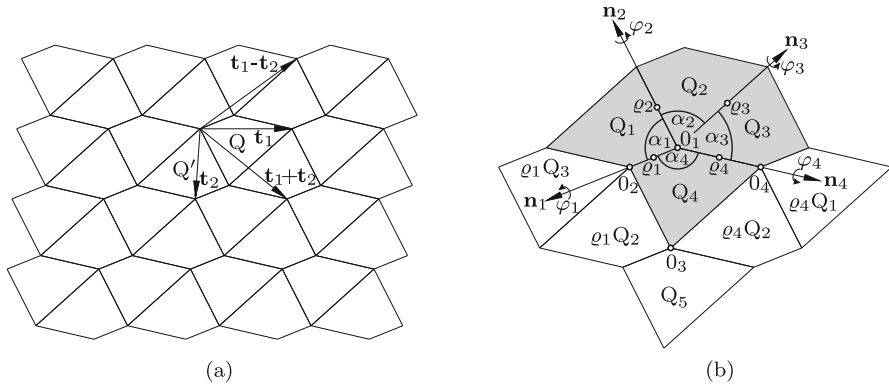


**Fig. 4.12** Tiling with irregular convex quadrilaterals (a) and clusters of four quadrilaterals (b)

(18.3). With cyclic permutations of indices the same equations relate other pairs of neighboring angles so that also  $\varphi_2$  and  $\varphi_3$  are determined as functions of  $\varphi_1$ . If  $(\varphi_1, \varphi_2, \varphi_3, \varphi_4)$  is a solution then, because of the symmetry to the plane, also  $(-\varphi_1, -\varphi_2, -\varphi_3, -\varphi_4)$  is a solution. In what follows,  $\varphi_1 > 0$  is assumed. The equations reveal the following facts. If  $\alpha_4$  is the largest of the four angles  $\alpha_1, \alpha_2, \alpha_3, \alpha_4$ , as is the case in the figure,  $\varphi_1, \varphi_2, \varphi_4 > 0$  and  $\varphi_3 < 0$  in one position and  $\varphi_1, \varphi_3, \varphi_4 > 0$  and  $\varphi_2 < 0$  in the other position.

These results are easily verified experimentally by folding a circular piece of paper along four radii having the directions of  $\mathbf{n}_1, \mathbf{n}_2, \mathbf{n}_3, \mathbf{n}_4$  (the four sectors should be made very stiff). It is also apparent that the cluster is immobile if the quadrilateral is nonconvex.

In what follows, it is assumed that in Fig. 4.12b the shaded cluster 1 is shown deformed in one of its two possible modes  $(\varphi_1, \varphi_2, \varphi_3, \varphi_4)$  with  $\varphi_1$  arbitrary. Let  $\varrho_i$  denote the tensor of the  $180^\circ$ -rotation about the axis through the midpoint of the edge common to  $Q_i$  and  $Q_{i-1}$  which is (i) normal to  $\mathbf{n}_i$  and (ii) bisecting the angle  $\pi - \varphi_i$  ( $i = 1, 2, 3, 4$  cyclic). The rotation  $\varrho_i$  transforms  $Q_i$  into  $Q_{i-1}$  and vice versa since a  $180^\circ$ -rotation equals its inverse. The short-hand notation of these relationships is

$$\left. \begin{aligned} Q_1 &= \varrho_1 Q_4, & Q_4 &= \varrho_1 Q_1 = \varrho_1 \varrho_2 Q_2, \\ Q_3 &= \varrho_4 Q_4, & Q_4 &= \varrho_4 Q_3 = \varrho_4 \varrho_3 Q_2 \end{aligned} \right\} \quad (4.40)$$

and, consequently,

$$\varrho_4 \varrho_3 = \varrho_1 \varrho_2. \quad (4.41)$$

By applying  $\varrho_1$  to the entire cluster 1 the overlapping congruent cluster 2 with center  $O_2$  and with new quadrilaterals  $\varrho_1 Q_2$  and  $\varrho_1 Q_3$  is obtained. Likewise, applying  $\varrho_4$  to cluster 1 the overlapping congruent cluster 4 with

center  $0_4$  and with new quadrilaterals  $\varrho_4 Q_1$  and  $\varrho_4 Q_2$  is obtained. Proposition: The three quadrilaterals  $\varrho_1 Q_2$ ,  $Q_4$  and  $\varrho_4 Q_2$  are obtained by subjecting  $Q_1$ ,  $Q_2$  and  $Q_3$ , respectively, to the rotation  $\varrho_2$  followed by the rotation  $\varrho_1$ , i.e.,  $\varrho_1 Q_2 = \varrho_1 \varrho_2 Q_1$ ,  $Q_4 = \varrho_1 \varrho_2 Q_2$ ,  $\varrho_4 Q_2 = \varrho_1 \varrho_2 Q_3$ . Proof: The first equation is true since  $Q_2 = \varrho_2 Q_1$ . The second equation is one of Eqs.(4.40). The third equation follows from  $\varrho_4 Q_3 = \varrho_4 \varrho_3 Q_4$  in combination with (4.41). End of proof. From this it follows that the cluster 3 formed by the quadrilaterals  $\varrho_1 Q_3$ ,  $Q_1$ ,  $\varrho_4 Q_3$  and  $Q_5$  with center  $0_3$  is also congruent with cluster 1 and that it is the result of the said rotations. By applying the same procedure successively infinitely many clusters can be added in all directions, all clusters being congruent with cluster 1 independent of the deformation of cluster 1. This ends the proof of mobility with degree of freedom one.

Taking  $\varrho_1$  as example, the  $180^\circ$ -rotations are expressed analytically as follows. It suffices to know the angle  $\varphi_1$  of the rotation  $(\mathbf{n}_1, \varphi_1)$  and the position vectors  $\mathbf{r}_i$  ( $i = 1, 2, 3$ ) of the corners  $0_1$ ,  $0_2$ ,  $0_3$  of  $Q_4$  in some arbitrarily chosen reference system. These data determine the midpoint  $\mathbf{r}_A = (\mathbf{r}_1 + \mathbf{r}_2)/2$  on the edge and the unit vector  $\mathbf{n}_1 = (\mathbf{r}_2 - \mathbf{r}_1)/|\mathbf{r}_2 - \mathbf{r}_1|$  of the rotation  $(\mathbf{n}_1, \varphi_1)$ . The auxiliary vector  $\boldsymbol{\varrho} = \mathbf{r}_3 - \mathbf{r}_1$  determines the unit vector  $\mathbf{e} = (\boldsymbol{\varrho} - \mathbf{n}_1 \mathbf{n}_1 \cdot \boldsymbol{\varrho})/|\boldsymbol{\varrho} - \mathbf{n}_1 \mathbf{n}_1 \cdot \boldsymbol{\varrho}|$  in the plane of  $Q_4$  and normal to  $\mathbf{n}_1$ . The vectors  $\mathbf{n}_1$  and  $\mathbf{e}$  and the angle  $\varphi_1$  determine the unit vector  $\mathbf{n}$  along the axis of the  $180^\circ$ -rotation  $\varrho_1$ :

$$\mathbf{n} = \mathbf{e} \sin \frac{\varphi_1}{2} - \mathbf{n}_1 \times \mathbf{e} \cos \frac{\varphi_1}{2}. \quad (4.42)$$

According to (3.17) the relationship between the positions  $\mathbf{r}$  and  $\mathbf{r}^*$  of an arbitrary point before and after the  $180^\circ$ -rotation  $\varrho_1$  is

$$\mathbf{r}^* = 2\mathbf{r}_A - \mathbf{r} + 2\mathbf{n} \mathbf{n} \cdot (\mathbf{r} - \mathbf{r}_A). \quad (4.43)$$

Formulas for the rotations  $\varrho_2$ ,  $\varrho_3$  and  $\varrho_4$  are obtained by cyclic permutation of indices.

## References

1. Bricard R (1926/27) Leçons de cinématique. v.I.: Cinématique théorique. v.II: Cinématique appliquée. Gauthier-Villars, Paris
2. Dimentberg F M (1948) A general method for the investigation of finite displacements of spatial mechanisms and certain cases of passive constraints (Russ.) Trudy Seminara po Teorii Mashin i Mechanismov, AN SSSR 5 Nr.17:5-39; Purdue Translation No.436, Purdue Univ.
3. Grübler M (1917) Getriebelehre. Eine Theorie des Zwanglaufes und der ebenen Mechanismen. Springer, Berlin
4. Kokotsakis A (1932) Über bewegliche Polyeder. Math. Ann.107,627-647
5. Pandrea N I (2000) Elemente de mecanica solidelor in coordonate Plückeriene. Editura Acad. Romane

6. Stachel H (2009) Remarks on Miura-Ori, a Japanese folding method. Proc. Int.Conf.Eng. Graphics and Design, TU Cluc-Napoca
7. Wittenburg J (1977) Dynamics of systems of rigid bodies. Teubner Stuttgart
8. Wittenburg J (2007) Dynamics of multibody systems. Springer, Berlin Heidelberg New York